

MOL 38901

**The unusual state-dependent affinity of P2X<sub>3</sub> receptors can be explained  
by an allosteric two-open-state model**

Karoly R, Mike A, Illes P, and Gerevich Z,

Department of Pharmacology, Institute of Experimental Medicine, Hungarian Academy of  
Sciences, Budapest, Hungary (R.K., A.M.)

Rudolf Boehm Institute of Pharmacology and Toxicology, Leipzig, Germany (P.I., Z.G.)

MOL 38901

Running title: Kinetics and affinity of P2X<sub>3</sub> receptors explained by model

Corresponding author: Mike A., Institute of Experimental Medicine, Hungarian Academy of Sciences, P.O. Box 67, H-1450 Budapest, Hungary

Tel: + 36 1 2109400, Fax: + 36 1 210 9423

E-mail: mike@koki.hu

**Number of figures: 6**

**Number of pages: 36**

**Number of references: 19**

**Number of words in *Abstract*: 242**

**Number of words in *Introduction*: 744**

**Number of words in *Discussion*: 1499**

**Nonstandard Abbreviations: HAD: high affinity desensitization; HEK: human embryonic kidney; hP2X<sub>3</sub>R: human P2X<sub>3</sub> receptor; meATP: methylene ATP; CTP: cytosine 5'-triphosphate; MWC: Monod-Wyman-Changeux**

MOL 38901

## ABSTRACT

High affinity desensitization (HAD) by nanomolar agonists was described to shape the ability of P2X<sub>3</sub> receptors for mediating pain sensation. These receptors are activated by micromolar ATP, but nanomolar ATP is sufficient to effectively desensitize them. The mechanism behind HAD is still obscure. It has been suggested, that HAD can only happen if the receptor has previously been activated and desensitized by high agonist concentrations. It was not clear, however, whether the high-affinity site was different from the conventional binding site, and which mechanism led to its exposure during desensitization. A subsequent paper argued that HAD could also occur without preceding desensitization, because even resting receptors expose high affinity binding sites. To support this hypothesis a kinetic model was proposed, which could reproduce all major phenomena observed experimentally. We attempted to improve this model, and used it to simulate the agonist-induced formation of the high affinity binding site. We collected electrophysiological data using HEK 293 cells expressing human P2X<sub>3</sub> receptors and fitted simulated currents to experimentally acquired currents. A simple allosteric kinetic model in which only triliganded receptors could open failed to reproduce receptor behavior introduction of an additional diliganded open state was necessary. Simulation with this model gave results which were in good agreement with experimental data. By using simulations and experiments we analyzed the process of high affinity binding site formation upon agonist exposure, and propose an explanation, which helps to resolve the apparent conflict regarding the mechanism of HAD.

MOL 38901

Rapid desensitization (within ~100 ms) and very slow recovery from desensitization (requiring several minutes) are the hallmark of P2X<sub>3</sub> (and also of P2X<sub>1</sub> (Rettinger and Schmalzing, 2003)) receptors (North, 2002). In the study of this phenomenon it has been shown that agonists compete for the same binding sites, and the recovery rate will be determined by the type of agonist occupying the binding sites of the receptors at the beginning of washout (Sokolova et al., 2004). Extremely low concentrations of agonists were found to be able to effectively inhibit agonist-evoked currents, presumably by inducing desensitization of the receptors. No detectable currents were evoked at these low concentrations, in fact a ~80 to 800-fold difference was found between IC<sub>50</sub> and EC<sub>50</sub> values of the same agonist.

The ability of low nanomolar agonist concentrations to induce desensitization was questioned by an elegant study of Pratt et al. (2005), where the ability of agonists to prevent recovery from desensitization was compared to their ability to induce desensitization. Intriguingly, and in contrast to previous results, no inhibition by nanomolar agonists was found without previous activation and desensitization.

Dealing with a mechanism, where agonists cannot induce desensitization, but once attained, they are able to stabilize desensitized conformation, presumes that equilibrium distribution of receptor states will be different, depending on the fact, whether receptors were in resting or in desensitized state at the beginning of low concentration agonist application. This idea is incompatible with classical models of receptor kinetics; a unique mechanism unlike the ones valid for other desensitizing receptors should have been proposed. However, no detailed hypothesis was offered for the mechanism by which this mysterious “transfiguration” of the binding sites occurred. Thus it is not clear, if formation of high affinity binding sites is supposed to be formation of novel sites, or reconstruction of existing

MOL 38901

ones. It is also unclear, why the authors had to suppose “rebinding” as a requirement of HAD (Pratt et al., 2005) (i.e., why staying bound would not suffice).

In a subsequent paper (Sokolova et al., 2006), a cleverly designed attempt was made to demystify HAD of P2X<sub>3</sub> receptors. In order to mechanistically explain findings with low concentration agonists, a kinetic model of the P2X<sub>3</sub> receptor was proposed. Simulations using this model adequately reproduced experimental data. By both experiments and simulation, the possibility of HAD even in the absence of preceding desensitization was demonstrated. However, the properties of the model used in this study cast doubt on this conclusion. Parameter optimization was probably done using a fitting algorithm, and the assumption of microscopic reversibility was not used as a constraint. The model predicts that unliganded receptors cannot open, they can only desensitize, diliganded receptors can neither desensitize nor open, while triliganded receptors can only desensitize via open state.

In order to be able to test hypotheses, gain more insight into the mechanisms of receptor activation and desensitization, and resolve contradicting results of previous publications, we decided it necessary to improve this model. We chose to construct an “allosteric” type of model (Monod et al., 1965), to ensure that it is thermodynamically feasible and as simple as possible (i.e., has few free parameters). In electrophysiological experiments we obtained kinetic data in a range of different concentrations, and used them to test different models. We started this approach with the simplest possible model, and increased the complexity only when it was proven to be necessary. A 10 state model with only eight free parameters reproduced all experimental data reasonably well.

Using electrophysiology and modeling the following specific questions were addressed:

- 1) Does increased affinity indeed require preceding agonist exposure?
- 2) Is the high-affinity site different from the conventional binding site?
- 3) Do we need to suppose unbinding and rebinding?
- 4) What is the mechanism of binding site “transfiguration”?
- 5) Do low

MOL 38901

concentration agonist-induced desensitization and recovery from desensitization converge to the same equilibrium distribution of receptors? (If they do, the conflicting views are simply due to the methodological problem of not perfusing the agonists long enough.) 6) Can a conventional allosteric model reproduce kinetic behavior of the receptor (in particular the extreme differences in the affinities of resting and desensitized conformations)?

Based on the simulations we were able to answer the above questions, and to propose an explanation of binding site "transfiguration", which resolves contradictions between previous experimental findings. We show that if we assume the simplest allosteric mechanism, increased affinity upon preceding agonist binding will unavoidably occur, and it does not require any unique mechanism.

MOL 38901

## MATERIALS AND METHODS

*Culturing of HEK293-hP2X<sub>3</sub> cells.* Methods of maintenance of HEK293 cells and their stable transfection with hP2X<sub>3</sub> cDNA have been described previously (Fischer et al., 2003). Cells were kept in Dulbecco's modified Eagle's medium (DMEM) also containing 25 mM HEPES, 110 µg/ml sodium pyruvate, 1 mg/ml D-glucose, 4 µg/ml pyridoxine (Life Technologies, Karlsruhe, Germany), 2 mM L-glutamine, 1% non-essential amino acids (NEAA) (all Sigma, Deisenhofen, Germany), 10% fetal bovine serum and 50 µg/ml geneticin (both from Life Technologies) at 37°C and 10% CO<sub>2</sub> in humidified air. They were plated on 35-mm plastic dishes (Sarstedt, Nürnberg, Germany) for electrophysiological recordings.

*Whole-cell patch-clamp recordings.* Whole-cell patch-clamp recordings were performed 2–6 days after the splitting of permanently transfected HEK293 cells at room temperature (20–22°C), using an Axopatch 200B patch-clamp amplifier (Molecular Devices, Union City, CA). Patch pipettes (3–5 MΩ) for HEK293 cells were filled with intracellular solution of the following composition (in mM): 135 CsCl, 2 MgCl<sub>2</sub>, 20 HEPES, 11 EGTA, 1 CaCl<sub>2</sub>, 1.5 Mg-ATP, and 0.3 Li-GTP, pH 7.3 adjusted with CsOH. The external recording solution consisted of (in mM) 140 NaCl, 5 KCl, 2 MgCl<sub>2</sub>, 2 CaCl<sub>2</sub>, 10 HEPES, and 11 glucose, pH 7.4 adjusted with NaOH. After the whole-cell configuration was established, an equilibrium period of 10 min was allowed to elapse for establishing adequate solution exchange between the patch pipette and the cell. All recordings were made at a holding potential of -70 mV. Data were filtered at 2 kHz, digitized at 5 kHz, and stored on a laboratory computer using a Digidata 1200 interface and pClamp 8.0 software (Molecular Devices).

Drugs were dissolved in external solution and applied by gravitation, locally to single cells, using a rapid solution exchange system (SF-77B Perfusion Fast-Step, Warner

MOL 38901

Instruments, Hamden, CT, USA). The 10-90% rise time of junction potential at open pipette tip was 1-4 ms.

*Materials and drugs.* The following pharmacological agents were used: adenosine 5'-triphosphate disodium salt (ATP),  $\alpha,\beta$ -methylene ATP lithium salt ( $\alpha,\beta$ -meATP),  $\beta,\gamma$ -methylene ATP ( $\beta,\gamma$ -meATP). All drugs were from Sigma, Deisenhofen, Germany and prepared as a concentrated stock solution in distilled water and were diluted to final concentration in external medium. Throughout this study (except when reproducing experiments with other agonists) we used  $\alpha,\beta$ -meATP as an agonist. The reason for this was to avoid interactions between P2Y and P2X<sub>3</sub> receptors. HEK293 cells express native G-protein coupled P2Y receptors, which are activated by the endogenous agonist, ATP. It has been shown that G protein-activation alters the rates of desensitization, and recovery from desensitization of P2X<sub>3</sub> receptors (Gerevich et al., 2005; Gerevich et al., 2007).

*Data analysis.* Data were analyzed off-line using pClamp 8.0 software (Molecular Devices). Figures show mean  $\pm$  SEM values of  $n$  experiments. Student's  $t$  test was used for statistical analysis. A probability level of 0.05 or less was considered to reflect a statistically significant difference.

*Simulations.* The simulation was based on a set of differential equations with the occupancy of each receptor state (i.e., the fraction of the receptor population in that specific state) given by the following equation:

$$\frac{dS_i(t)}{dt} = \sum_j^n S_j(t) * k_{ji} - S_i(t) * k_{ij}$$



MOL 38901

where  $S_i(t)$  is the occupancy of a specific state at the time  $t$ .  $S_j(t)$  is the occupancy of a neighboring state. Neighboring states are states where direct transitions are possible.  $n$  is the number of neighboring states,  $k_{ij}$  and  $k_{ji}$  are the rate constants of transitions between neighboring states.

All simulations were performed using Berkeley Madonna v8.0.1 (<http://www.berkeleymadonna.com/>) to solve the differential equations using fourth-order Runge-Kutta method. All parameters were fitted manually.

MOL 38901

## RESULTS

### *Does equilibrium distribution of receptor states depend on the initial distribution?*

The first question to be answered was whether equilibrium distribution of receptor states indeed depended on their initial distribution as it had been proposed. If this were the case, there would be more than one equilibria, and thus the mechanism would not be compatible with traditional kinetic models; therefore there would be no point in trying to develop an acceptable one.

To study this question, we investigated the kinetics of recovery from desensitization, and the development of HAD in the presence of nanomolar agonist concentration (10 nM  $\alpha,\beta$ -meATP). After a pulse of 10  $\mu$ M  $\alpha,\beta$ -meATP, 10 nM of the same agonist was superfused for different periods of time (Fig. 1A). Although a single exponential equation does not properly describe the recovery process (see below), the dominant component of recovery could be determined by fitting a single exponential function to the data. The time constant was found to be 309.3 s (Fig.1B). This time constant should be similar to the time constant of the onset of desensitization in the presence of 10 nM  $\alpha,\beta$ -meATP, since both depend on the same rate constants. We chose to test the 32 min interval, since this is more than five times the apparent time constant. Thus – supposing an exponential time course – the distribution of receptors must be within 1% of the equilibrium distribution. After a 32 min perfusion of 10 nM  $\alpha,\beta$ -meATP the availability of receptors was tested (using a 10 s pulse of 10  $\mu$ M of the agonist). We found that the presence of preceding agonist pulse did not change the equilibrium, the availability was virtually identical ( $p = 0.98$ , paired t test,  $n = 6$ ), irrespectively of the presence or absence of a preceding agonist pulse (Fig.1C).

MOL 38901

*Concentration dependence of current onset and decay at low agonist concentrations*

In order to construct a model that can reproduce the kinetics of channel behavior throughout an agonist concentration range of several orders of magnitude (from nanomolar to micromolar), it was crucial that reliable records of various concentrations of agonists were available. Measurement of current kinetics can be done most accurately at low agonist concentrations, where activation is slow, therefore is not limited by the properties of the drug application system, furthermore currents are small, therefore are not distorted by series resistance error. We used a heterologous expression system in order to make sure that kinetics of low concentration-evoked currents can be properly measured, and are not contaminated by heteromeric P2X<sub>2/3</sub> receptor-mediated currents (these receptors are also activated by  $\alpha,\beta$ -meATP, but have slower kinetics). We measured currents evoked by the following concentrations of  $\alpha,\beta$ -meATP: 100, 178, 316, 562, 1000, 1780 and 3160 nM (Fig. 2). Agonist pulses were given every 5 minutes. Experiments were started by repeated applications of 316 nM of  $\alpha,\beta$ -meATP, to ensure the stability of current amplitudes. Once this was established, 316 nM  $\alpha,\beta$ -meATP was applied alternating with other concentrations, and served as a control throughout the experiment: Each evoked current was normalized to the average of the two neighboring control currents. The amplitude of 316 nM  $\alpha,\beta$ -meATP-evoked currents was fairly stable throughout the experiment; for currents evoked within the first hour of recording, the normalized standard deviation was  $0.076 \pm 0.031$ . However, the time constant of current decay increased with recording time monotonically, changing by  $54.8 \pm 9.9\%$  ( $n = 6$ ) in an hour. (For all control currents evoked within the first hour the normalized standard deviation was  $0.19 \pm 0.07$ ). This change, however, was within the cell-to-cell variance of decay time constants (the normalized standard deviation of which was 0.41), and we did not study its origin. Fig. 2 illustrates different concentration-evoked currents recorded from a cell. Currents evoked by each concentration were acquired from at least five cells, the averaged traces were

MOL 38901

used to fit the onset and decay kinetics of simulated currents. The concentration-response curve, based on peak amplitudes, yielded an  $EC_{50}$  of 1.29  $\mu$ M, with an  $n_H$  of 1.34.

### *Construction of the model*

As Sokolova et al.(2006) convincingly argued, the behavior of P2X<sub>3</sub> receptors is best described by a circular model where binding of three agonist molecules is allowed (which is consistent with the trimeric structure of the receptor (Nicke et al., 1998)). We, therefore, used the scheme of their model as a starting point. Since we have no structural information suggesting that distinct submolecular regions (gates) would be responsible for activation and desensitization, we simplified their scheme, and omitted the rapidly developing desensitized state “A<sub>3</sub>D<sub>f</sub>” (Fig. 3A).

In the case of a circular scheme the simplest possible way to construct a model is to use the allosteric model of oligomeric proteins as described by Monod, Wyman and Changeux (Monod et al., 1965). By identifying our model as of “Monod-Wyman-Changeux-type” (MWC-type), or “allosteric”, we mean that it fulfills the following three main conditions (for a more comprehensive description of allosteric models see (Colquhoun, 1998; Karpen and Ruiz, 2002)): 1) The model is based on the concept that agonists can bind to different conformational states of the receptor, but with different affinities. 2) the ratio of affinities is equal to the ratio of gating equilibria with  $n$  vs.  $n+1$  bound agonists (determined by the “ratio constant” ‘ $x$ ’, as described below). 3) Subunits of the receptor change their conformation in a concerted way.

The first assumption seems to be reasonable and well-founded in the case of most receptors. As for the second condition, we consider it as a way to reduce the number of free parameters (e.g. from 17 to 8 in the case of our starting model shown in Fig. 3A), and as a

MOL 38901

way to maintain microscopic reversibility. If MWC-type models constructed using this condition are able to reproduce experimental data well, it will not be a proof that the actual behavior of the receptor agrees with this assumption. The third assumption (i.e., there are no mixed-conformation receptors; e.g. one subunit open – two subunits closed) is almost certainly not true for the actual behavior of receptors, nevertheless, we chose to introduce this simplification, since models without this constraint did not reproduce experimental data significantly better, while unnecessarily complicated the scheme of conformations.

For constructing a full allosteric model (Fig.3A) eight parameters had to be defined (see also Table 1): the concentration-independent term ('a') of association rate constants (' $k_i$ '), the dissociation rate constant (' $l_1$ '), rate constants of desensitization and recovery of the vacant receptor (' $d_0$ ' and ' $r_0$ '), opening ('o') and closing ('c') rate constants, rate constant of the open-to-desensitized transition ('od'), and a "ratio constant" ('x'). The calculated parameters are listed in Table 1.

The ratio constant determined both the ratio of affinities to desensitized vs. resting receptors, and the ratio of equilibrium desensitization values with n vs. n+1 bound agonist molecules. We found that the model reproduces receptor behavior better if we choose the rate of association to be independent of the conformation (i.e.,  $k_i = m_i$ ), and make the rate of dissociation determine preferential affinity to desensitized receptors alone (see Fig. 3A). Using these principles, all other rate constants ( $k_1, k_2, k_3, l_2, l_3, m_1, m_2, m_3, n_1, n_2, n_3, d_2, d_3, d_4, r_2, r_3, r_4$ ) except reopening from desensitization ('do') can be derived, as shown in Fig.3A, and microscopic reversibility will be maintained. Reopening from desensitization is calculated from rate constants o, c, od, d<sub>4</sub> and r<sub>4</sub>.

The opening rate constant ('o') was taken from Sokolova et al.(2006). We did not attempt to construct a model that reproduces single channel behavior. Single channel activity was found to be too fast to be resolved, and there was no evidence for a single conductance state

MOL 38901

(Evans, 1996). Due to these difficulties, no dwell time histograms are available so far, and the origin of fast flickering single channel activity is not known. Therefore, the only limitation for 'op' was to be high enough to allow fast activation at high agonist concentrations. Flash photolysis of 100  $\mu$ M caged ATP resulted in an activation with a 20 to 80 % rise time of 20 ms (Grote et al., 2005). This is quite consistent with the rate constant given by Sokolova et al. (2006).

The closing rate constant ('c') was chosen to be higher than in the paper by Sokolova et al. (2006). Although proper single channel analysis has not been performed for P2X<sub>3</sub> receptors, we can suppose from nonstationary fluctuation analysis data (Grote et al., 2005) that maximal open probability is not higher than ~0.6 to 0.8.

Rate constant of desensitization from open state ('od') was determined based on the results of Sokolova et al. (2006), where half times of desensitization converged to ~50 ms at high agonist concentrations.

We introduced a ratio constant ('x') which determined both the ratio of affinities to desensitized vs. resting receptors and the increase in equilibrium desensitization due to the binding of an agonist. For the sake of flexibility we initially defined three different ratio constants ('x', 'y' and 'z') to different binding steps. From the simulations (not shown) we later found that having the same constant for all three agonist binding steps was sufficient.

For the determination of the rate constants of desensitization ('d') and recovery ('r'), we had two clues: 1) Rate of recovery was dependent on the agonist, therefore isomerization of the vacant receptor cannot be rate limiting (or can only be in the case of the agonist showing the fastest dissociation, which was CTP). Therefore, the rate of D to R isomerization ('r') must be at least ~0.1 in order to allow recovery from CTP-bound desensitized state rapidly enough (Pratt et al., 2005). 2) We can safely suppose, that in the absence of agonists most receptors are in resting state, therefore 'd' should not be higher than ~0.1.

MOL 38901

Dissociation rate constants ( $k_{-1}$ ) were determined based on the recovery time constants, supposing that isomerization of vacant receptors is faster, therefore dissociation from the desensitized receptor ( $n_1$ ) is rate limiting. From  $n_1$   $k_{-1}$  can be determined using  $x$  (Fig.3A).

The model constructed this way reproduced experimentally acquired behavior of the receptors rather poorly. In order to find an optimal set of parameters, we started with optimizing  $a$  for current onset rates at different  $x$  values. Since at low concentrations association must be the rate limiting step, the rate of association can be estimated sufficiently well. The best  $a$  values for  $x = 5, 10, \text{ and } 20$ , were 7.5, 1.5, and 1.4, respectively (see Table 1). Fig.3B illustrates normalized experimentally obtained currents evoked by 516 nM  $\alpha, \beta$ -meATP, and simulated currents. At  $x = 5$  and 10 the current did not desensitize properly (a large plateau current remained). At  $x = 20$ , although the kinetics was sufficiently well reproduced, the magnitude of currents was extremely small (the maximal occupancy of open state was  $\sim 0.014$ ; note the scale of the right Y axis). The concentration-response curve at  $x = 20$ ,  $a = 1.4$  was shifted to the right: the  $EC_{50}$  was 17  $\mu\text{M}$  (Fig.3C).

When we tried to bring concentration-response curves close to experimental values by increasing  $a$  values (Fig.3D), the onset kinetics became much faster than in experimental data (Fig.3E).

The problem, as we understood, was the following: We know from the decay time constants at high agonist concentration that desensitization from open state is fast ( $\tau \approx 50$  ms; see Fig1C in Sokolova et al. (2006)). If we suppose only one open state ( $A_3O$ ), then open receptors will isomerize into desensitized conformation with the same rate, irrespective of the overall occupancy of the binding sites in the whole receptor population. For this reason, agonists at low concentration will not evoke significant current, since receptors reach open

MOL 38901

state at a low rate, while desensitize at a constant, high rate. Therefore, in order to reproduce experimental data, we need slower desensitization from open state at a lower agonist occupancy level. This is only possible if we suppose at least one additional open state with a slower desensitization rate. Thus low agonist concentrations could evoke a relatively large current with slow kinetics, as observed experimentally.

In our next model, therefore, we added an open state of diliganded receptors, and initially supposed that diliganded receptors open and close with the same rates as triliganded ones ( $o_2 = o_3$  and  $c_2 = c_3$ ). Since the  $d_2 / r_2$  ratio differs from the  $d_3 / r_3$  ratio, ' $od_2$ ' and ' $do_2$ ' must also differ from ' $od_3$ ' and ' $do_3$ ' in order to preserve microscopic reversibility; they are calculated as:  $od_2 = od_3 / x$ , and  $do_2 = do_3 * x$  (Fig.4A).

As seen in Table 1, value of ' $a$ ' only needed a slight adjustment, while ' $x$ ' remained the same. Rate constants of desensitization and recovery from desensitization of the vacant receptor (' $d_0$ ' and ' $r_0$ ') were optimized by fitting the concentration-HAD curve (see Fig.4C).

Figure 4B illustrates experimental and simulated agonist-evoked currents at four agonist concentrations: 100, 178, 316, and 562 nM. Concentration-HAD and concentration-peak amplitude curves are shown in Fig. 4C, illustrating data from Pratt et al. (2005), Sokolova et al. (2006), and our current experiments ( $n = 4$  to 8 for each point). (The reason why concentration-HAD curves in the two previous publications differ so much will be discussed below.)

#### *Formation of the high affinity binding site*

A special test revealed a peculiar behavior of P2X<sub>3</sub> receptors (Pratt et al., 2005). In a special protocol; which we will call the 'early-late' protocol, control agonist pulse and test



MOL 38901

pulse were separated by a long interpulse interval. In either the first- or the second half of the interpulse interval, nanomolar agonist was perfused. P2X<sub>3</sub> receptors behaved in a remarkably counter-intuitive way: nanomolar agonists caused weak inhibition when applied in the second half of the interpulse interval (i.e., right before the test pulse), but (the same concentration of agonist, for the same duration) caused a much stronger inhibition when it was applied in the first half (right after the control pulse), even though in this case availability was tested only after a long recovery period.

Nanomolar agonist perfusion during the first half of the interpulse interval was intended to cause inhibition of the test current by stabilizing desensitization, while perfusion during the second half by inducing desensitization. The fact, that the inhibition caused by the early pulse was much more effective, indicates that low concentration of the agonist was able to bind to a high-affinity site, which is accessible upon desensitization, but becomes inaccessible as recovery from desensitization progresses.

We intended to understand what mechanism can be responsible for this unexpected phenomenon. We started with analyzing a single step within the protocol: the sequence of events taking place during an exchange of agonists. We simulated replacement of a high concentration rapidly dissociating agonist with a low concentration slowly dissociating agonist.

We assumed three binding sites at each receptor, with identical association and dissociation rates for all three sites. No cooperativity of binding was assumed. Since the questions addressed by these simulations are of qualitative nature, the exact values of rate constants are of no importance. The same qualitative results were produced with different types of models, and using different parameters, if the following assumptions were made (in accordance with the model of Sokolova et al.(2006)): 1) With one of the binding sites occupied, most receptors desensitize. 2) With all three binding sites unoccupied, most

MOL 38901

receptors recover from desensitized state. 3) The affinity of agonists to desensitized state is much larger than to resting state, which is reflected by a much slower dissociation from desensitized state. 4) Isomerization of vacant receptors from desensitized to resting conformation is relatively fast (i.e., during recovery from desensitization the rate limiting step is dissociation, not isomerization). 5) The rate of agonist association is determined by agonist concentration, and at the studied concentration-range (~1 to 100 nM) it is comparable with the dissociation rate. 6) The rate of agonist dissociation is agonist-dependent, for some agonists (e.g.  $\beta,\gamma$ -meATP) dissociation is faster than for others (e.g.,  $\alpha,\beta$ -meATP).

In order to be able to perform simulations of agonist association and dissociation dynamics with two agonists, we made one additional assumption: 7) Isomerization rates (resting to desensitized and desensitized to resting transition rates) are dependent only on the number of bound agonists and not on which agonist occupies individual binding sites.

Rate constants for the simulations using the scheme shown in Fig.5A were taken from the model described above (Fig. 4A). Horizontal and vertical transitions show association and dissociation of 'drug B' and 'drug A', respectively. Desensitized states (subunits marked by circles) are shown in the front, resting states (subunits marked by squares) are in the back. In order to help comparison, states of Fig. 4A (without open states) are marked by the shaded area. Since this scheme was designed for the study of equilibration at nanomolar agonist concentration, where no significant opening occurs, open states are ignored. Furthermore, since in this specific experiment, when replacement of a rapidly dissociating agonist by a low concentration slowly dissociating agonist is studied, many of the states shown in Fig. 5A do not reach a significant occupancy, and thus can be ignored. Figure 5B shows only the states which are relevant in this experiment. (Ignoring the rest of the states does not mean not calculating with them, they are ignored only in the illustration, and solely for the sake of clarity.) All shown states reached an occupancy above 0.01 at some time during this

MOL 38901

simulation experiment, while ignored states never exceeded the occupancy value 0.0001 at any time.

For specific parameters used in this simulation see Table 1. Effects of two fictitious drugs, called ‘drug A’ (a slowly dissociating agonist) and ‘drug B’ (a rapidly dissociating agonist) were simulated. In the experiments illustrated here, parameters of ‘drug A’ were equivalent with parameters of  $\alpha,\beta$ -meATP as used in the simulations shown in Fig. 4. Parameters (association and dissociation rate constants) of the rapidly dissociating agonist, ‘drug B’ were chosen so that it roughly reproduced recovery kinetics of  $\beta,\gamma$ -meATP, but the microscopic affinity was chosen to be the same as in the case of  $\alpha,\beta$ -meATP (i.e., the ratio of ‘a’ and ‘ $l_1$ ’ was kept constant – see Table 1), so that the effect of difference in association- and dissociation kinetics could be studied separately, not disturbed by a difference in affinity.

Fig.5C illustrates availability of the receptor population as a function of time for three cases: 1) Simple association of ‘drug A’ molecules at a concentration of 10 nM (black line). 2) 10  $\mu$ M of ‘drug B’ (rapidly dissociating) replaced by 10 nM of ‘drug A’ (slowly dissociating): Dissociation of ‘drug B’ and association of 10 nM of ‘drug A’ (dark gray line). 3) 10  $\mu$ M of ‘drug A’ replaced by 10 nM of ‘drug A’: Development of the new equilibrium (light gray line). The process we want to analyze is the second case.

During progressive dissociation of ‘drug B’ and association of ‘drug A’ receptors are kept in desensitized conformation provided that at least one of the binding sites is occupied. Desensitized conformation is characterized by a higher agonist affinity, therefore more ‘drug A’ molecules associate in this state, than to resting receptors. Relative occupancy values of states are illustrated at five different times (2s, 10s, 20s, 40s, and 1200s after replacement of 10  $\mu$ M ‘drug B’ by 10 nM ‘drug A’ (Fig.5D). During dissociation of ‘drug B’ association of ‘drug A’ is already started (see 2s at Fig. 5D), and while a fraction of receptors loses all its ‘drug B’ molecules and directly reaches resting vacant state, the majority of receptors will

MOL 38901

have one or two ‘drug A’ molecules bound by the time the last ‘drug B’ molecule dissociates (see 40s at Fig. 5D). Since one bound agonist is enough to keep the receptor in high affinity state, association of ‘drug A’ molecules will continue to occur in spite of the low concentration, unless the receptor momentarily loses all three agonists. Whenever this happens, there is a fair chance that isomerization (D to R transition) occurs sooner than a new association. Once the receptor is isomerized into the low affinity resting conformation, affinity becomes much less, and most resting receptors remain unoccupied. This way the pool of high affinity (agonist-bound, desensitized) receptors is slowly drained, and receptors accumulate in the vacant resting state (see 1200s at Fig. 5D). At equilibrium a small fraction of resting vacant receptors still binds a single agonist molecule, and among these unliganded resting receptors some may desensitize before dissociation. Thus, the final equilibrium will be predominantly determined by the two slowest reactions: association of the first ‘drug A’ to the vacant low affinity resting state (this reaction is slow because of the low concentration and the low affinity); and dissociation of the last ‘drug A’ from the unliganded high affinity desensitized state (this reaction is slow because of the high affinity of desensitized receptors). Both isomerization reactions are faster.

#### *The ‘early-late’ protocol tested in simulations and experiments*

Having proposed a mechanism of high affinity binding site formation, and the sequence of events during agonist exchange we analyzed the mechanisms behind the ‘early-late’ protocol.

We simulated the effects of the two agonists mentioned above: ‘drug B’ (rapidly dissociating) and ‘drug A’ (slowly dissociating). First of all, we simulated the rate of recovery from desensitization after ‘drug B’ and ‘drug A’ application for comparison (Fig. 6A). Then,

MOL 38901

different interpulse intervals, as well as different combinations of agonists were tested. (By interpulse interval we mean the time between control and test pulses – illustrated by black triangles in Fig. 6B.) During either the first (‘early’) or the second (‘late’) half of the interpulse interval 10 nM of ‘agonist A’ is applied; for illustration see Fig. 6B.) The effect of different interpulse intervals is shown in Fig. 6B. The dynamics of receptor availability is illustrated by pairs of thin lines for four different interpulse intervals (100, 200, 300, and 400 s; illustrated by the bars below the figure). Lines increasing monotonously in their second section show receptor availability during the ‘early’ protocol, while lines decreasing in their second section show availability during the ‘late’ protocol. Final availability right before the test pulse (of high concentration agonist) is illustrated by diamonds (‘early’ drug application) and squares (‘late’ drug application); simulations were performed with interpulse intervals increasing from 0 to 400 s. It is apparent from the figure, that increased potency upon ‘early’ application is only observable within a definite time window (0 to 175 s in this case). Since this time window is determined by the ratio of dissociation rates of the two agonists, it is logical to presume that the paradoxical increased potency upon ‘early’ application will not occur when different concentrations of a single agonist are used. Figure 6C illustrates the plot of final availability as a function of interpulse duration in the case of both ‘drug A’ (filled symbols) and ‘drug B’ (open symbols): No matter how long interpulse duration was chosen, ‘early’ application never caused larger inhibition than ‘late’ application. This seems logical, since in both ‘early’ and ‘late’ protocols: 1) equal time was provided for dissociation of the agonist, therefore similar degree of dissociation is expected, and 2) equal time was provided for equilibration in the presence of low concentration agonist; which in the case of ‘early’ application means dissociation, while in the case of ‘late’ application means association.

As a general conclusion, our simulations suggested, that the experiment was only able to produce the unexpected increased potency upon ‘early’ application, if two conditions were

MOL 38901

met: 1) non-equilibrium conditions (i.e., drug application and recovery times had to be short enough as compared to the rate of equilibration; and 2) a rapidly dissociating agonist had to be replaced by a slowly dissociating one.

This prediction, that it is impossible to achieve larger inhibition with ‘early’ agonist application when a single agonist is used was tested experimentally as well. When we repeated the ‘early-late’ experiment using 100  $\mu\text{M}$   $\beta,\gamma\text{-meATP}$  and 10 nM ATP, or 100  $\mu\text{M}$   $\beta,\gamma\text{-meATP}$  and 50 nM  $\alpha,\beta\text{-meATP}$ , our results clearly reproduced previous findings of Pratt et al. (2005) and Sokolova et al. (2006). However, when the same agonist was used (10  $\mu\text{M}$   $\alpha,\beta\text{-meATP}$ , and 50 nM  $\alpha,\beta\text{-meATP}$ ), the ‘late’ application of the low concentration agonist caused larger inhibition (Fig. 6D).

MOL 38901

## DISCUSSION

P2X<sub>3</sub> receptors desensitize within milliseconds, but require several minutes to recover from desensitization. They are activated by micromolar-, while effectively desensitized by nanomolar agonist concentrations (Pratt et al., 2005; Sokolova et al., 2004; Sokolova et al., 2006). Both phenomena originate from the activation and desensitization mechanisms of the receptors, which, however, have not so far been clarified. We aimed to answer some specific questions regarding the mechanism by which P2X<sub>3</sub> receptors work and produce the peculiar phenomena described in the quoted papers. Answering most questions required not only electrophysiological experiments (in which only conducting and nonconducting states can be separated), but also the additional insight provided by simulations, in which the dynamics of all major conformational states, as well as different degrees of agonist occupancy can be monitored, and thus gating mechanism of real receptors can be explored.

The validity of conclusions drawn from simulations obviously depends on whether the model adequately reflects the actual mechanism of receptor activation and desensitization. The fact that the model sufficiently well reproduces all experimental findings (concentration dependence of activation rate, decay rate, current amplitude and HAD as well as recovery rate from desensitization), does not prove this. There are many uncertain points regarding the mechanism of activation and desensitization: Since single channel properties of P2X<sub>3</sub> receptors preclude a proper analysis (Evans, 1996), the number of coupled open and closed states, as well as the actual rate constants cannot be determined. Nevertheless, some conclusions regarding the feasible mechanisms by which P2X<sub>3</sub> receptors work, still can be drawn.

One conclusion comes from the observation, that no matter what type of model we tested, addition of a diliganded open state was necessary to adequately reproduce experimental data.

MOL 38901

This suggests that a significant fraction of diliganded receptors is likely to reach open conformation. Diliganded open state is characterized by a lower desensitization rate, which means that in case of prolonged agonist application low concentration can be as effective as high concentration in terms of cumulative charge flux. A study of mutated heterotrimeric P2X<sub>2/3</sub> receptors suggests that receptors can open from a less than fully liganded state (Wilkinson, 2006). Our findings – obtained by a different approach – suggest that this applies to homomeric P2X<sub>3</sub> receptors as well.

Another significant conclusion is that although it seems paradoxical that ‘early’ application of nanomolar agonist is more effective than ‘late’ application, this finding can be conveniently explained by supposing that binding of one agonist molecule increases the affinity of the second and third binding sites. If we assume this, the “paradoxical” behavior emerges whenever: 1) the interpulse interval is short enough, i.e., the experiment is done under non-equilibrium conditions; and 2) a rapidly dissociating agonist is exchanged to a slowly dissociating one.

In the light of the results of electrophysiological and simulation experiments we can answer the questions posed in the Introduction:

1) Does increased affinity indeed require preceding agonist exposure?

Yes and no. Although our model suggests that vacant resting receptors have no high affinity binding sites, occasional binding nonetheless can happen even at nanomolar agonist concentration. Whenever binding happens, there is a chance (~5 % in our model) that it results in receptor desensitization before dissociation, i.e. high affinity binding sites are formed. Once desensitized, dissociation is less-, while association is more probable, thus receptors will slowly accumulate in desensitized states. Slowly though, but the final equilibrium will be reached. The rate of equilibration indeed will be considerably higher when



MOL 38901

previous agonist exposure brings receptors into desensitized (i.e., high affinity) states, as illustrated in Fig. 5C (black vs. dark gray lines), thus in this sense preceding agonist exposure does enhance high affinity binding. The affinity of pre-exposed desensitized and non-pre-exposed desensitized receptors, however, will be the same, and so will be the final equilibrium in both experiments. It was observed that a slowly dissociating agonist seems to be by far more effective in an experimental protocol where it is given during pulses of a rapidly dissociating agonist than when given without previous activation (see Fig. 6 in Pratt et al (2005)). This difference does not arise from reaching different equilibria depending on the initial condition, but from approaching equilibria at completely different rates. The apparent difference in affinity exists only under non-equilibrium conditions.

2) Is the high-affinity site different from the conventional binding site?

No, in this model the same binding site has different affinities in different conformations (resting or desensitized) of the receptor.

3) Do we need to suppose unbinding and rebinding?

No, in the model, association of a single agonist molecule is enough to induce desensitization, and thus to produce high affinity binding sites. Having three agonist binding sites per receptor, agonist exchange can take place in a subunit-by-subunit manner, without full dissociation, as shown in Fig. 5D. Unbinding and rebinding, therefore, does occur, but mostly not on the level of receptors, only on the level of receptor subunits. Thus, contrary to what was assumed by Pratt et al. (2005), the desensitized-to-resting isomerization does not need to be slow.

4) What is the mechanism of binding site “transfiguration”?

No special mechanism is needed. If we simply assume that agonists have a higher affinity to desensitized receptors, and that binding of one single agonist is able to bring the receptor

MOL 38901

into desensitized state, high affinity binding sites will be formed upon association of the first agonist molecule.

5) Do low concentration agonist-induced desensitization and recovery from desensitization converge to the same equilibrium distribution of receptors?

Yes. If enough time is provided for the equilibrium to develop, there will be no difference in the degree of inhibition depending on the starting distribution of receptor conformations, as we have demonstrated by experiments (Fig. 1), and simulations (Fig. 5C). The rate of equilibration is determined by both agonist association and dissociation, therefore it is lowest at very low concentrations (recovery from desensitization in the presence of 10 nM  $\alpha,\beta$ -meATP proceeded with a time constant of 309 s) Supposing single exponential decay, one must wait roughly  $5 \cdot \tau$  in order to approach the equilibrium within  $\pm 1\%$ , which is  $\sim 25$  min in this case. This is the reason why durations of low concentration agonist application chosen by both Pratt et al.(2005) (60 s for recovery) and Sokolova et al. (2006) (90 s for association) were by far too short, and thus represent non-equilibrium conditions. This also explains why their HAD vs. concentration curves differ so much (Fig. 4C). In our experiments (Fig. 1) we started with assessing the time needed for equilibration and then chose a duration of agonist application which assured that equilibrium is adequately approached.

6) Can a conventional allosteric model reproduce kinetic behavior of the receptor?

Yes. In fact we needed a very simple model to accomplish this. There was no need to assign different ratio constants to different binding steps, no need to introduce “cooperativity of binding”, and no need to suppose non-concerted isomerizations of subunits.

The principal question of course is not what experiments tell about the properties of the model (i.e., if we can construct a model that reproduces experimental data), but what the

MOL 38901

model tells about the object of our experiments (i.e., whether our model helps to understand the mechanism behind the properties of the receptor).

Sokolova et al. (2006) argued convincingly, that a proper model of the P2X<sub>3</sub> receptor must be circular, and should have three binding sites. In this paper we add, that beside the triliganded open state, a diliganded open state must also be assumed, and that a simple allosteric mechanism can adequately describe the behavior of the receptor, including some phenomena, which so far have been unexplained, such as the several hundredfold difference between IC<sub>50</sub> and EC<sub>50</sub> values, the several thousand fold difference between time constants of desensitization and recovery, and the formation of high affinity binding sites upon previous agonist exposure. The fact that a MWC-type model so simply explains and so readily reproduces experimentally obtained phenomena, however, certainly does not prove that receptors indeed activate and desensitize by this mechanism, i.e., that subunits of the receptor change their conformation in a concerted manner. Non-concerted isomerization of subunits has been proven in a number of ion channels (e.g. (Chapman et al., 1997; Rosenmund et al., 1998; Ruiz and Karpen, 1997)). However, in the case of P2X<sub>3</sub> receptors, we must suppose, that partial occupancy of agonist binding sites drastically increases the affinity of the rest of (non-occupied) binding sites, otherwise no model could reproduce experimental behavior. The MWC model is not the only-, but the simplest way to explain increased affinity of non-occupied binding sites of partially occupied receptors. One possible alternative mechanism is, that although single-subunit isomerizations can happen, neighboring subunits affect each other. Isomerization of a single subunit due to agonist binding may increase the probability of isomerization of neighboring subunits, thus affecting the affinity of their binding sites (as it was supposed in the sequential model of Koshland et al. (1966)). Further experimental and modeling data will help to refine the molecular mechanisms involved in P2X<sub>3</sub> receptor gating.

MOL 38901

### **ACKNOWLEDGEMENTS**

We thank Dr. Rashid Giniatullin for his helpful comments on this manuscript.

MOL 38901

## REFERENCES

- Chapman ML, VanDongen HM and VanDongen AM (1997) Activation-dependent subconductance levels in the drk1 K channel suggest a subunit basis for ion permeation and gating. *Biophys J* **72**:708-19.
- Colquhoun D (1998) Binding, gating, affinity and efficacy: the interpretation of structure-activity relationships for agonists and of the effects of mutating receptors. *Br J Pharmacol* **125**:924-47.
- Evans RJ (1996) Single channel properties of ATP-gated cation channels (P2X receptors) heterologously expressed in Chinese hamster ovary cells. *Neurosci Lett* **212**:212-4.
- Fischer W, Wirkner K, Weber M, Eberts C, Koles L, Reinhardt R, Franke H, Allgaier C, Gillen C and Illes P (2003) Characterization of P2X<sub>3</sub>, P2Y<sub>1</sub> and P2Y<sub>4</sub> receptors in cultured HEK293-hP2X<sub>3</sub> cells and their inhibition by ethanol and trichloroethanol. *J Neurochem* **85**:779-90.
- Gerevich Z, Zadori Z, Müller C, Wirkner K, Schröder W, Rubini P, Illes P. (2007) Metabotropic P2Y receptors inhibit P2X<sub>3</sub> receptor-channels via G protein-dependent facilitation of their desensitization. *Br J Pharmacol*. **151**:226-236.
- Gerevich Z, Müller C, Illes P. (2005) Metabotropic P2Y<sub>1</sub> receptors inhibit P2X<sub>3</sub> receptor-channels in rat dorsal root ganglion neurons. *Eur J Pharmacol*. **521**:34-38.
- Grote A, Boldogkoi Z, Zimmer A, Steinhauser C and Jabs R (2005) Functional characterization of P2X<sub>3</sub> receptors fused with fluorescent proteins. *Mol Memb Biol* **22**:497-506.
- Karpen JW and Ruiz M (2002) Ion channels: does each subunit do something on its own? *Trends Biochem Sci* **27**:402-9.
- Koshland DE, Jr., Nemethy G and Filmer D (1966) Comparison of experimental binding data and theoretical models in proteins containing subunits. *Biochemistry* **5**:365-85.
- Monod J, Wyman J and Changeux JP (1965) On the Nature of Allosteric Transitions: A Plausible Model. *J Mol Biol* **12**:88-118.
- Nicke A, Baumert HG, Rettinger J, Eichele A, Lambrecht G, Mutschler E and Schmalzing G (1998) P2X<sub>1</sub> and P2X<sub>3</sub> receptors form stable trimers: a novel structural motif of ligand-gated ion channels. *EMBO J* **17**:3016-28.
- North RA (2002) Molecular physiology of P2X receptors. *Physiol Rev* **82**:1013-67.
- Pratt EB, Brink TS, Bergson P, Voigt MM and Cook SP (2005) Use-dependent inhibition of P2X<sub>3</sub> receptors by nanomolar agonist. *J Neurosci* **25**:7359-65.
- Rettinger J and Schmalzing G (2003) Activation and desensitization of the recombinant P2X<sub>1</sub> receptor at nanomolar ATP concentrations. *J Gen Physiol* **121**:451-61.
- Rosenmund C, Stern-Bach Y and Stevens CF (1998) The tetrameric structure of a glutamate receptor channel. *Science* **280**:1596-9.
- Ruiz ML and Karpen JW (1997) Single cyclic nucleotide-gated channels locked in different ligand-bound states. *Nature* **389**:389-92.
- Sokolova E, Skorinkin A, Fabbretti E, Masten L, Nistri A and Giniatullin R (2004) Agonist-dependence of recovery from desensitization of P2X<sub>3</sub> receptors provides a novel and sensitive approach for their rapid up or downregulation. *Br J Pharmacol* **141**:1048-58.
- Sokolova E, Skorinkin A, Moiseev I, Agrachev A, Nistri A and Giniatullin R (2006) Experimental and modeling studies of desensitization of P2X<sub>3</sub> receptors. *Mol Pharmacol* **70**:373-82.
- Wilkinson WJ, Jiang L-H, Surprenant A, and North RA (2006) Role of ectodomain lysines in the subunits of the heteromeric P2X<sub>2/3</sub> receptor *Mol Pharmacol* **70**:1159–1163,

MOL 38901

## FOOTNOTES

This work was supported by grants from the Deutsche Forschungsgemeinschaft (IL 20/11-3) and the Hungarian Research Fund (T 037659) A.M. is recipient of a Janos Bolyai Research Fellowship.

MOL 38901

## LEGENDS FOR FIGURES

Figure 1. Equilibrium value of receptor availability in the presence of low agonist concentration. **A)** Superimposed traces show an example of 10  $\mu\text{M}$   $\alpha,\beta\text{-meATP}$ -evoked currents in a cell. First current is an example of control currents (having maximal availability), subsequent currents were evoked after application of 10 nM  $\alpha,\beta\text{-meATP}$  for 1, 2, 4, 8, 16 or 32 minutes. Four of the currents are shown on an expanded time scale (upper panel). Each individual current is normalized to the average of the two control currents evoked before and after it (for this reason, a vertical scale bar is not shown). **B)** Averaged values of recovery from desensitization in the presence of 10 nM  $\alpha,\beta\text{-meATP}$  ( $n = 5$ ). Control currents were evoked before each test by a 10s pulse of 10  $\mu\text{M}$   $\alpha,\beta\text{-meATP}$ , then 10 nM  $\alpha,\beta\text{-meATP}$  was perfused for one of the following durations: 1, 2, 4, 8, 16 or 32 minutes, after which the availability of receptors was tested by another 10s pulse of 10  $\mu\text{M}$   $\alpha,\beta\text{-meATP}$ . Five minutes were allowed for recovery between tests. Data were fitted by a monoexponential function;  $\tau = 309.3$  s. **C)** Inhibition by 10 nM  $\alpha,\beta\text{-meATP}$  applied for 32 minutes. No difference in final equilibria was found depending on the initial condition, i.e., between receptors fully desensitized initially by a pre-pulse of 10  $\mu\text{M}$  of  $\alpha,\beta\text{-meATP}$  (Pre), and between receptors in initial resting state (NoPre).

Figure 2. Currents evoked by the application of  $\alpha,\beta\text{-meATP}$  at different concentrations ranging from 100 nM to 3.16  $\mu\text{M}$ . Inset shows normalized current traces in order to illustrate concentration-dependent changes in onset- and decay kinetics.

Figure 3. Simulations using the simplest (one-open-state) model of  $\text{P2X}_3$  receptors. **A)** Scheme #1 shows the one-open-state model. 'R' – resting states; 'D' – desensitized states; 'O'

MOL 38901

– open state; ‘A’ indicates agonist bound states, the number following it indicating the number of bound agonists. Transition rate constant, and their calculation are shown next to the arrows. **B)** Simulation of 562 nM  $\alpha,\beta$ -meATP application with different values of the parameter ‘x’. The corresponding parameter ‘a’ was determined for each ‘x’ by fitting the onset rate of simulated currents to the onset phase of experimentally acquired currents (regardless of the simulated current amplitude). Gray traces: simulated currents. Black traces: average (n = 5) of experimentally acquired 562 nM  $\alpha,\beta$ -meATP-evoked currents. Values of ‘x’ and ‘a’ were ‘x’ = 5; 10; 20 and ‘a’ = 7.5; 1.5; 1.4, respectively. Note the scale of both Y axes: The model with parameters x = 20, a = 1.4 seemed to reproduce the currents shape, but with an extremely low amplitude. **C)** Concentration-response curve simulated using the parameters ‘x’ = 20, ‘a’ = 1.4. The concentration-response curve is strongly shifted to the right when parameters were determined based on the kinetics and final equilibrium of 562 nM  $\alpha,\beta$ -meATP-evoked currents. Black diamonds show the experimentally measured-, gray squares the simulated concentration-response curve. **D)** When ‘a’ was determined based on concentration-response data, ‘a’ = 16 reproduced current amplitudes best. **E)** Simulation of currents using these parameters (‘x’ = 20, ‘a’ = 16) failed to reproduce the kinetics.

**Figure 4.** Simulations using the revised (two-open-state) model of P2X<sub>3</sub> receptors. **A)** Scheme #2 shows the two-open-state model. An additional diliganded open state was added. Formulas show the calculation of rate constants for the new transitions. Rate constants for the rest of the transitions are calculated as in the one-open-state-model (see. Fig. 3A). **B)** Experimentally acquired (black traces; average of n = 5) and simulated (gray traces) currents evoked by four different concentrations of  $\alpha,\beta$ -meATP (100, 178, 316 and 562 nM). **C)** Concentration-response curves, and concentration-HAD curves obtained in three different experimental studies and in simulations. Thick black lines: simulated data. Thin lines: Experimental data



MOL 38901

obtained by Pratt et al. (2005) (light gray, triangles), Sokolova et al. (2006) (dark gray, circles) and in this current study (black, diamonds). While concentration-response curves are close to each other, concentration-HAD curves differ considerably because of insufficient equilibrium in the experiments of Pratt et al. (2005) (started from fully desensitized receptors; 60 s for equilibration) and Sokolova et al. (2006) (started from resting receptors, 90 s for equilibration). In our current study (open diamonds) we let the receptors equilibrate in the presence of nanomolar concentrations of  $\alpha,\beta$ -meATP for 960 s, which was proven to be enough for equilibration. Simulations were performed using a 2000s equilibration period for all concentrations.

**Figure 5.** Simulation of agonist exchange on the receptor binding sites. **A)** The full model of agonist exchange. Circles and squares represent desensitized and resting receptor conformation, respectively. Open symbols represent subunits with unoccupied binding site, while filled symbols represent occupied binding sites (black – ‘drug B’, gray – ‘drug A’). Horizontal and vertical transitions represent association and dissociation of ‘drug B’ (rapidly dissociating) and ‘drug A’ (slowly dissociating), respectively. Diagonal transitions represent isomerization of the receptor. Resting and desensitized states which correspond to those of Scheme #1 and #2 are within the encircled area. **B)** Calculation of rate constants shown in the simplified scheme of the model. Association of ‘drug B’ is not shown, since this was not studied in this particular simulation. States which have not been visited by at least 0.01 % of the receptors at any time during the experiment are ignored for better visibility. All shown states have been visited by more than 1 % of the receptor population at some time during the experiment. Rate constants: ( $n_A, n_B$  –dissociation rate constant for ‘drug A’ and ‘drug B’ in desensitized conformation;  $m_A$  – association rate constant of ‘drug A’ in desensitized conformation;  $l_A$  – dissociation rate constant for ‘drug A’ in resting conformation;  $k_A$  –

MOL 38901

association rate for ‘drug A’ in resting conformation;  $d_0$ ,  $d_1$  -desensitization rate constants at 0 and 1 occupied binding sites, respectively;  $r_0$ ,  $r_1$  – rate constant of recovery from desensitization at 0 and 1 occupied binding sites, respectively;  $[A]$  –concentration of ‘drug A’.) **C)** Change of receptor availability in the presence of 10nM of ‘drug A’ with different initial conditions Black line – no previous desensitization; light gray line – after full desensitization by the same drug (‘drug A’); dark gray line – after full desensitization by ‘drug B’. X marks show times where occupancy of states is illustrated in panel D. **D)** The sequence of dissociation and association steps taking place during simulation of replacement of ‘drug B’ by ‘drug A’ is illustrated by the relative occupancy values of different states at different time intervals (2, 10, 20, 40 and 1200 seconds, also shown by X marks in panel C) after drug exchange. The overall availability during this simulation is illustrated by the dark gray line in panel C.

**Figure 6.** Simulation of “Early-Late” protocol using the two-agonist model shown in Fig. 5.

**A)** Simulated recovery from inactivation in case of ‘drug B’ (a rapidly dissociating fictitious drug with dissociation kinetics similar to  $\beta,\gamma$ -meATP), and ‘drug A’ (a slowly dissociating fictitious drug, with properties similar to  $\alpha,\beta$ -meATP). After removal of ‘drug B’, receptors recover within ~100 seconds, while after ‘drug A’ recovery takes ~300-400 seconds.

**B)** Simulations show changes in receptor availability during the ‘early-late’ protocol, illustrating that there is a definite time window for the peculiar phenomenon (of early agonist application causing larger inhibition than late agonist application) to develop.

High concentration ‘drug B’ applications (control and test pulses) are marked by black triangles in the lower panel. At time zero ‘drug B’ is removed, all receptors are in a fully liganded desensitized state, from which recovery starts. In the case of ‘early’ protocol recovery initially proceeds in the presence of 10 nM of ‘drug A’. It is of moderate rate, and

MOL 38901

converges to the equilibrium availability in the presence of 10 nM of ‘drug A’. In the case of the ‘late’ protocol, recovery starts in the absence of agonists, therefore it is rapid and full.

Solid lines illustrate availability in the case of four different interpulse intervals, (illustrated below the graph). Perfusion of 10 nM of ‘drug A’ was simulated either during the first (‘early’ protocol), or the second (‘late’ protocol) half of the interpulse interval. Availability at the end of the interpulse interval is illustrated by diamonds (‘early’ protocol), or squares (‘late’ protocol) in 40 different cases (interpulse intervals ranging from 10 to 400 s)

**C)** Simulations with different concentrations of a single agonist. The same drug (‘drug B’ – open symbols; ‘drug A’ – closed symbols) was used both at high concentration to evoke initial desensitization and at low concentration to evoke high affinity desensitization. Availability at the end of the interpulse interval is plotted as the function of interpulse interval duration. Simulations illustrate that ‘late’ application always produces larger inhibition when a single agonist is used. **D)** Inhibition by “early” and “late” application of agonists at low concentrations. Experiments were performed using 10  $\mu\text{M}$   $\alpha,\beta$ -meATP versus 50 nM  $\alpha,\beta$ -meATP; 100  $\mu\text{M}$   $\beta,\gamma$ -meATP versus 10 nM ATP and 100  $\mu\text{M}$   $\beta,\gamma$ -meATP versus 50 nM  $\alpha,\beta$ -meATP. Lower panel shows examples of the currents acquired. Horizontal scalebars: 1 s; vertical scalebars: 0.1 nA (left), 0.4 nA (middle) and 0.6 nA (right). Interpulse interval was determined to match the time required for recovery: 300s in the case of  $\alpha,\beta$ -meATP, and 120 s in the case of  $\beta,\gamma$ -meATP. Similarly to simulations, ‘early’ application only resulted in larger inhibition when a rapidly dissociating agonist was replaced by a slowly dissociating one. Asterisks indicate the level of significance.

MOL 38901

**Table 1.**

Parameters used in simulations using Scheme #1 (see Fig. 3), Scheme #2 (see Fig. 4), and the Two-agonist scheme (see Fig. 5 and 6)

	Scheme #1.	Scheme #2.	Two agonist scheme	
			Drug A	Drug B
a	1.4	1.3	1.3	9.75
$l_1$	0.5	4	4	30
$d_0$	0.002	0.003	0.003	
$r_0$	2.25	0.07	0.07	
o	65	65	-	
c	10	10	-	
od	20	20	-	
x	20	20	20	

**Fig. 1**

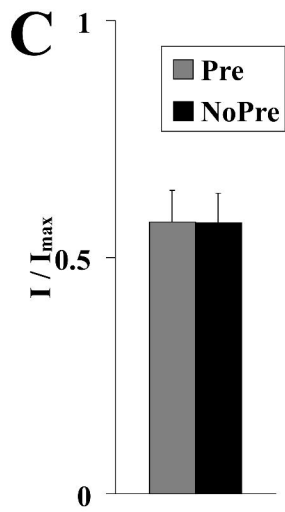
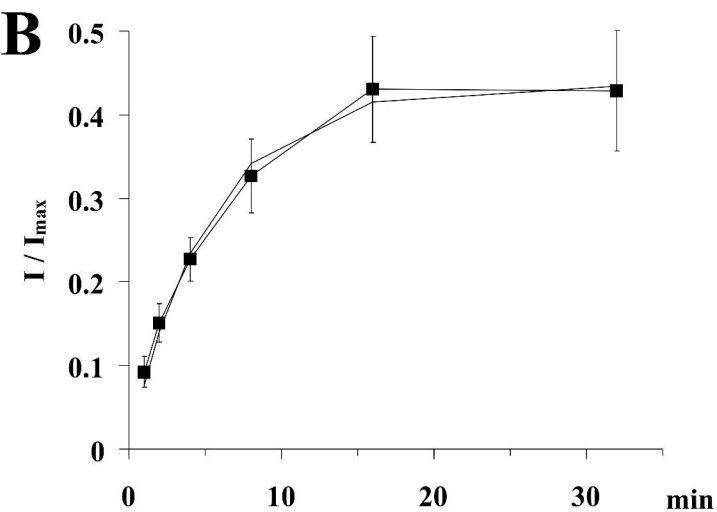
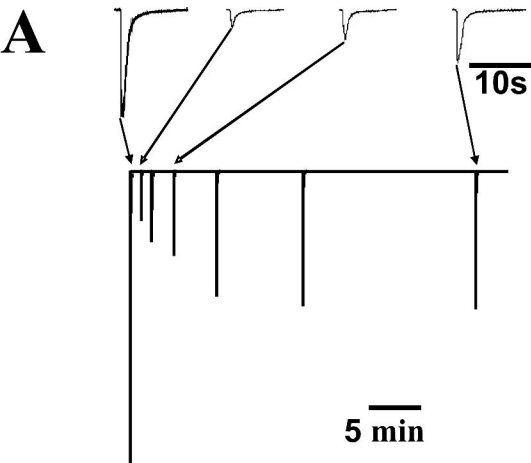
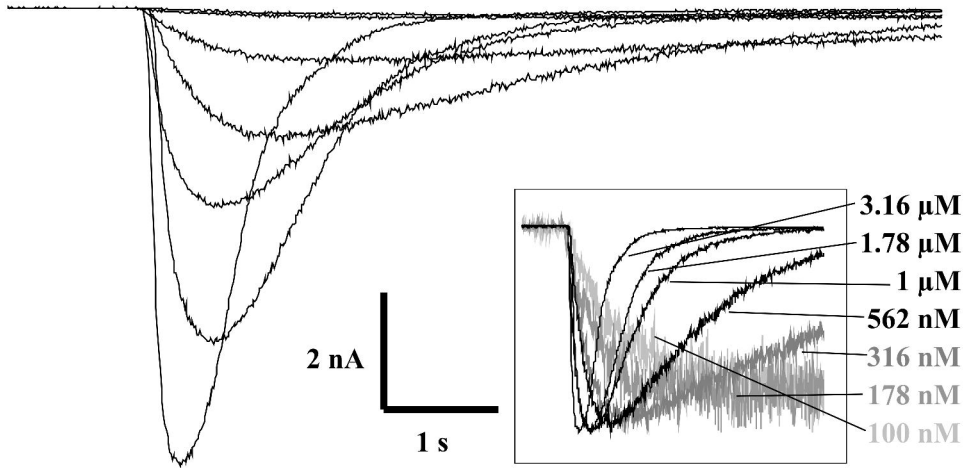
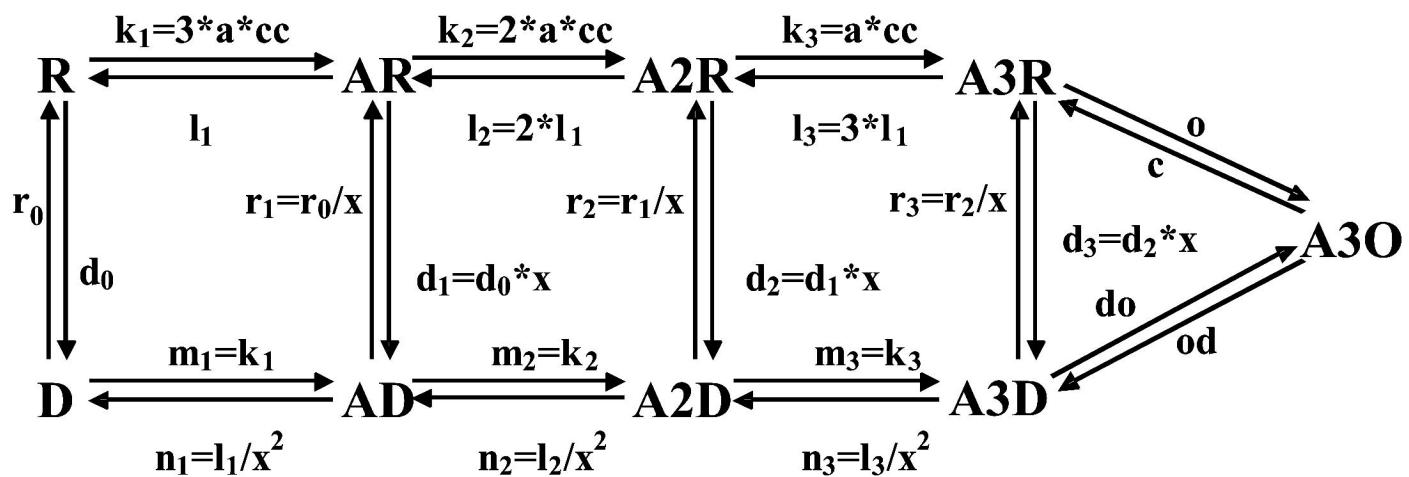


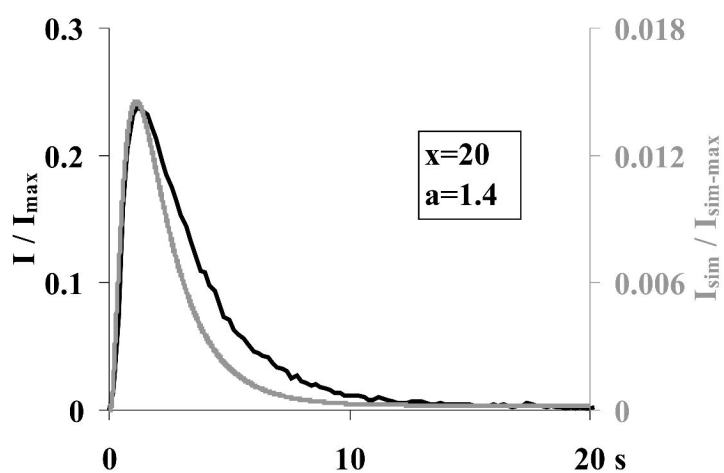
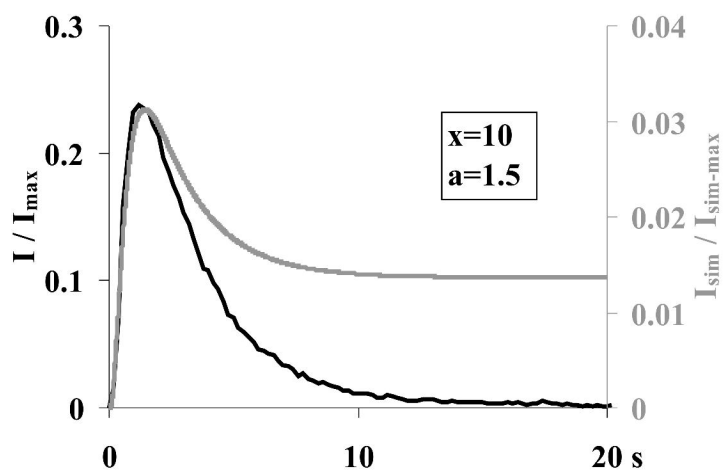
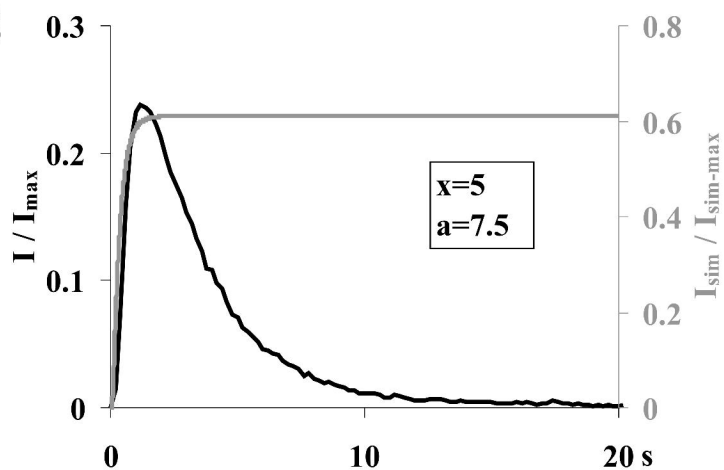
**Fig. 2**



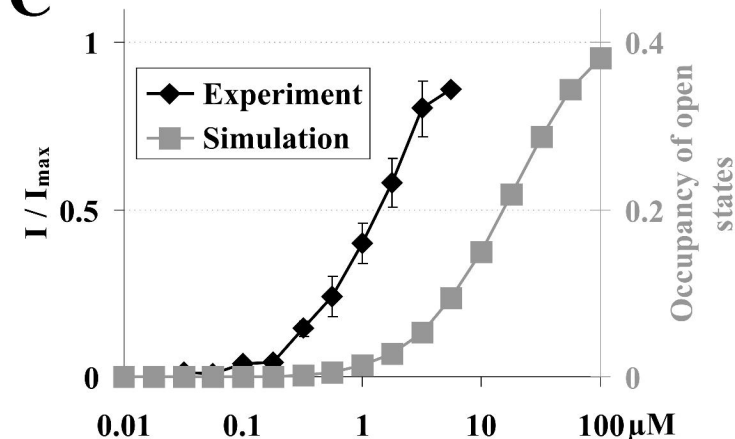
**A**



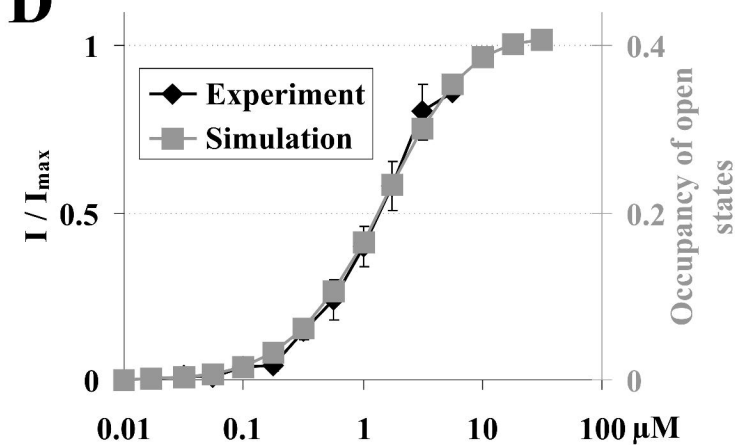
**B**



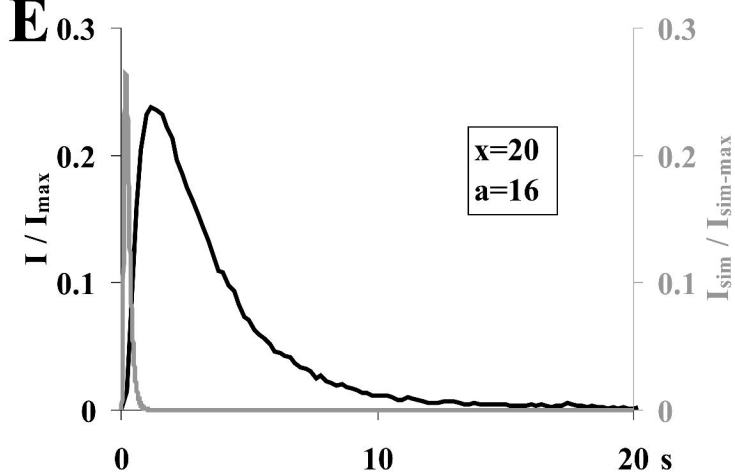
**C**

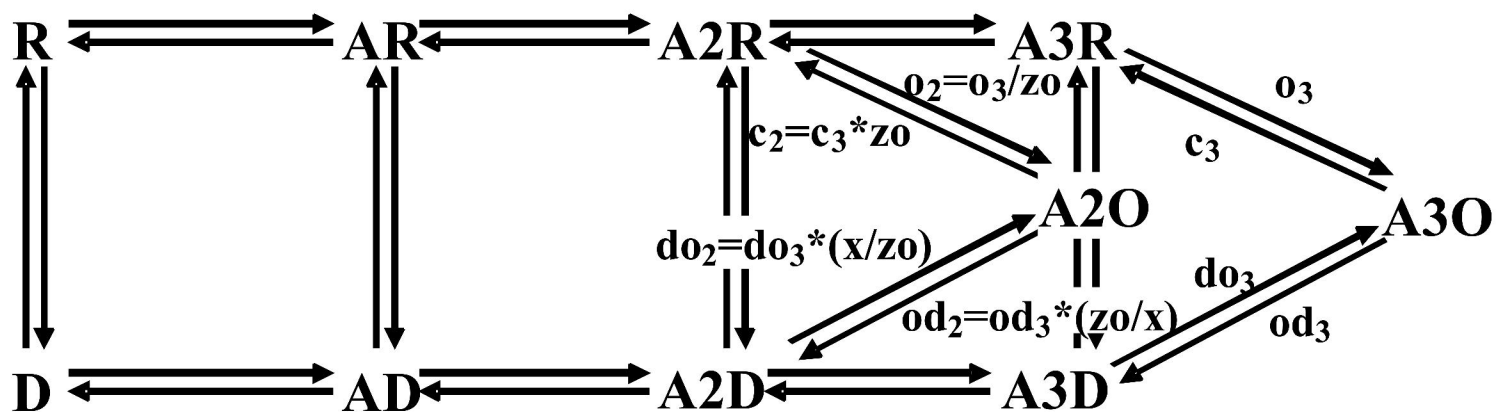
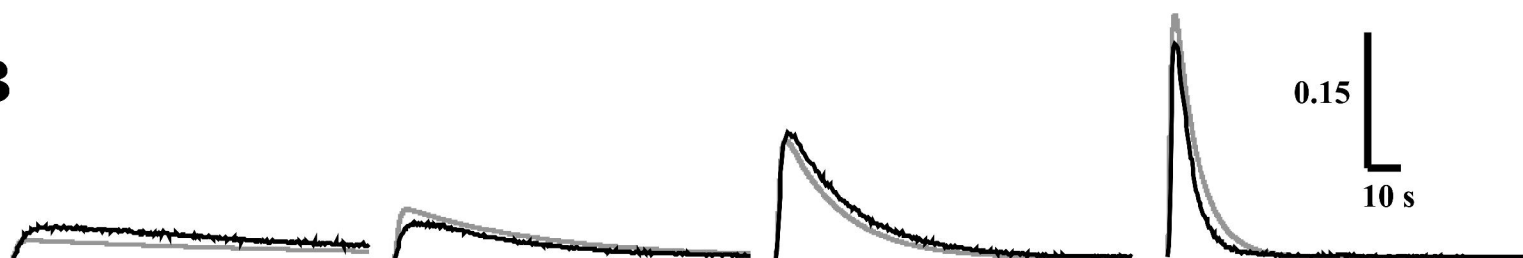
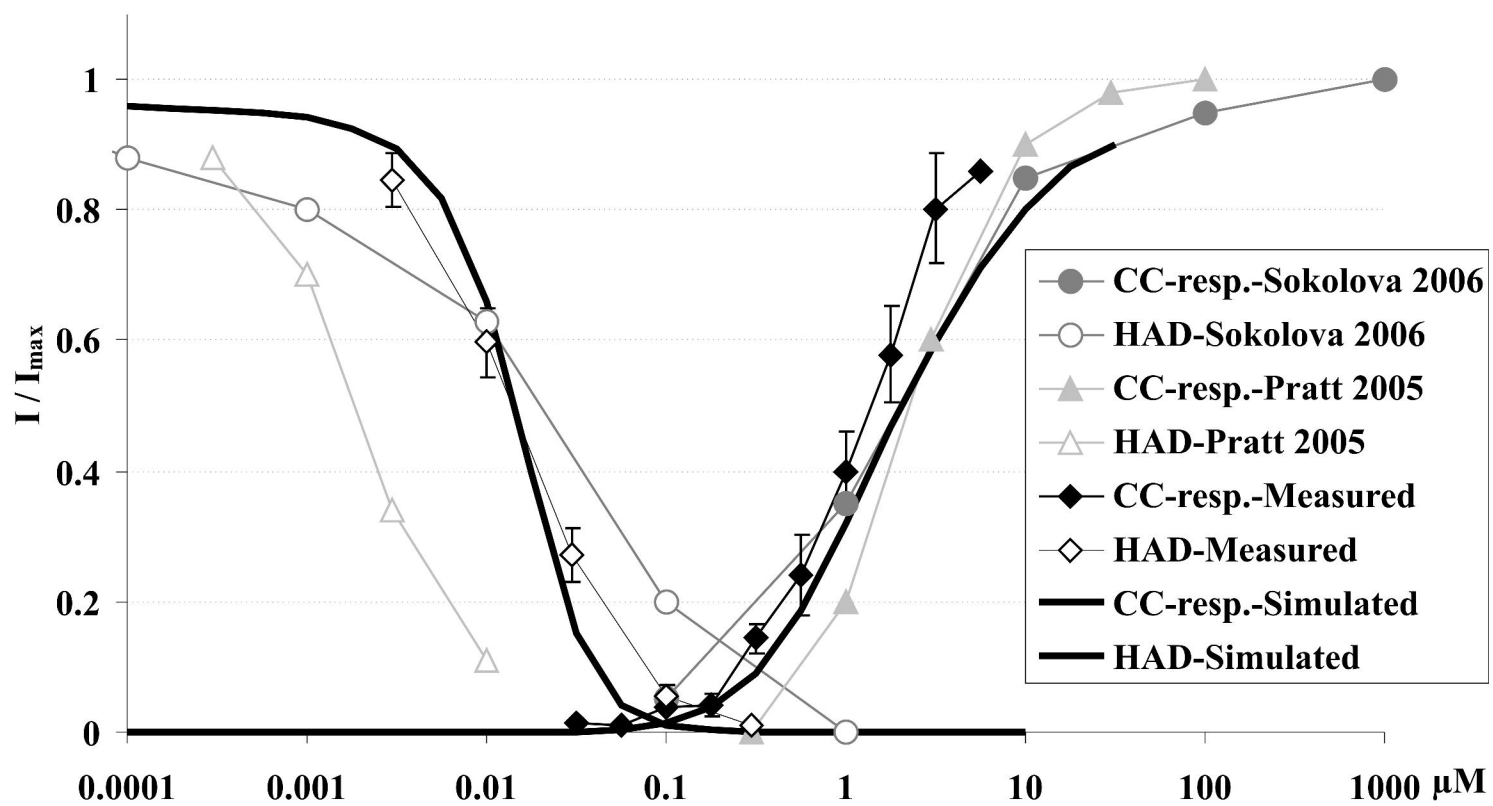


**D**



**E**



**Fig. 4****A****B****C**



**Fig. 5**

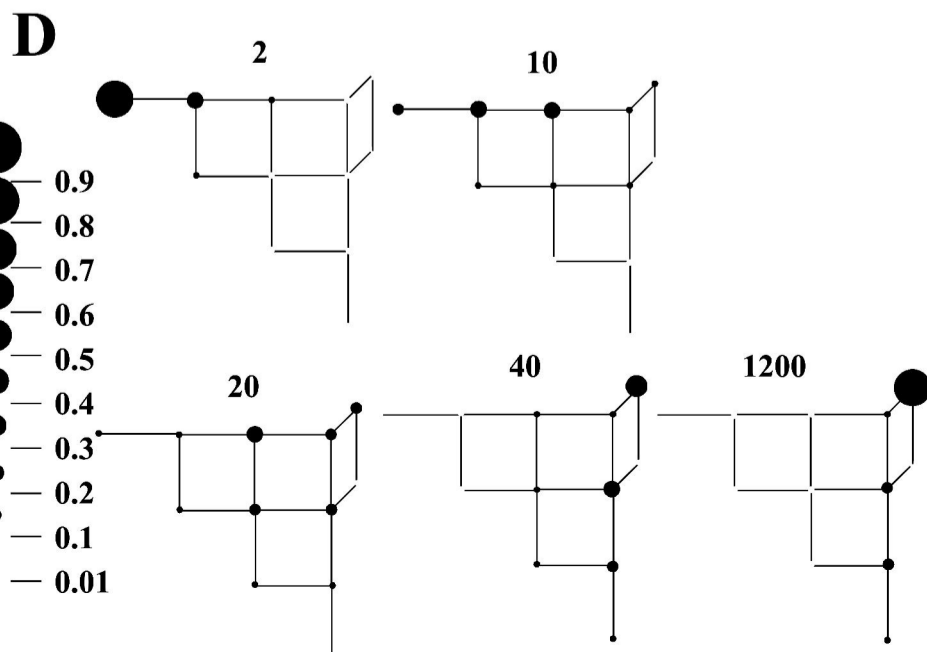
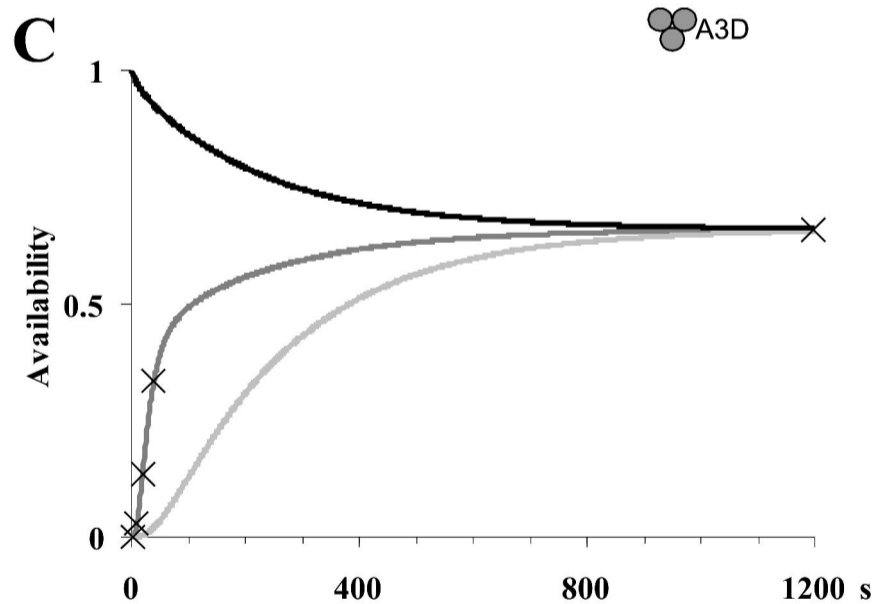
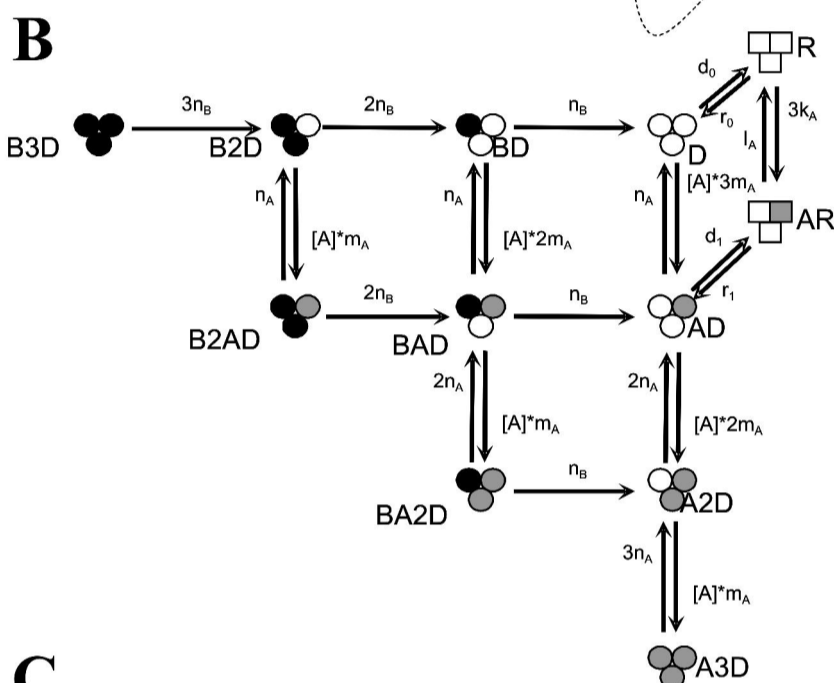
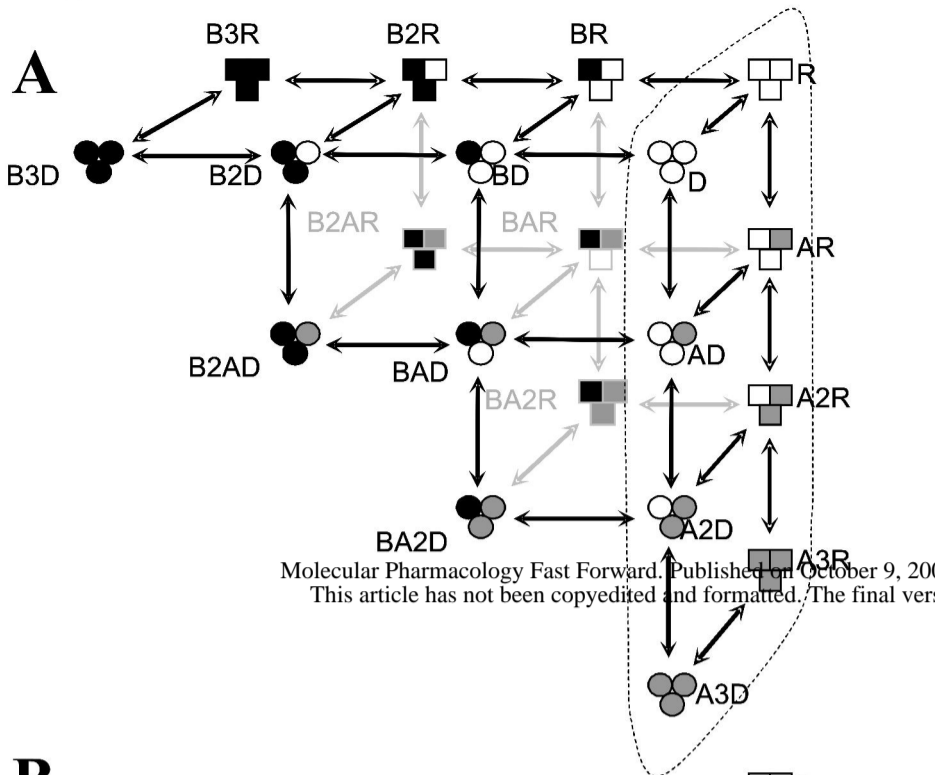


**Fig. 6**